JJMIE

Jordan Journal of Mechanical and Industrial Engineering

Volume 11 Number 1, January. 2017
ISSN 1995-6665
Pages 1 -11

Performance Assessment and Theoretical Simulation of Adsorption Refrigeration System Driven by Flat Plate Solar Collector

Raed Al-Rbaihat [a], Ahmad Sakhrieh [b,c,*], Jamil Al-Asfar [c,d], Ali Alahmer [a], Osama Ayadi [c], Ahmed Al-Salaymeh [c], Zayed Al_hamamre [e], Abeer Al-bawwab [f], Mohammed Hamdan [c]

[a] *Department of Mechanical Engineering, Al-Tafila Technical University, P. O. Box 179, 66110 Al-Tafila, Jordan*
[b] *Department of Mechanical and Industrial Engineering, American University of Ras Al Khaimah, 10021 UAE*
[c] *Mechanical Engineering Department, The University of Jordan, Amman 11942, Jordan*
[d] *Deoartment of Mechanical Engineering, Al-Zaytoonah University of Jordan, Amman 11733 Jordan*
[e] *Chemical Engineering Department, The University of Jordan, Amman 11942, Jordan*
[f] *Department of Chemistry, The University of Jordan, Amman 11942, Jordan*

Received JUNE, 20, 2016 *Accepted OCT, 10, 2016*

Abstract

The performance of an 8.0 kW Solar Adsorption Refrigeration System (SARS) under Jordanian climate conditions was evaluated experimentally and theoretically. The solar cooling system under study consists of four subsystems, namely silica gel/water adsorption chiller, solar thermal collector, cooling tower and fan coil unit. The ambient temperature, global solar radiation, relative humidity, wind speed and the temperatures of the solar adsorption system at different locations of experimental setup were measured.

Simulation of the solar adsorption system was carried out using the TRaNsientSYstem Simulation software (TRNSYS). The solar adsorption system is based on adsorption chiller operated by hot water produced by flat plate solar collectors with a total surface area of 41m2.

The obtained results revealed chilling power and thermal COP of 4.5 kW and 0.34, respectively when the average chilled water outlet temperature, cooling water inlet temperature, and hot water inlet temperatures were 16.8 °C, 28.1°C and 80.2 °C, respectively.

Keywords: *Adsorption system, solar, Silica gel/water, COP, TRNSYS simulation*.

Nomenclatures

Notation	Description	Unit
THW-in	Temperature of the hot water at the chiller inlet	°C
TCW-in	Temperature of the cooling water at the chiller inlet	°C
TCHW-in	Temperature of the chilled water at the chiller inlet	°C
THW-out	Temperature of the hot water at the chiller outlet	°C
TCW-out	Temperature of the cooling water at the chiller outlet	°C
TCHW-out	Temperature of the chilled water at the chiller outlet	°C
$\dot{m}$	Water flow rate	kg/s
SARS	Solar adsorption refrigeration system	
HMCSR	Hamdi Mango Center for Scientific Research	
TRNSYS	TRaNsientSYstem Simulation software	
HCFC	Hydrchlorofluorocarbon	
CFC	Chlorofluorocarbons	
F	Fraction of adsorption chiller rated value	
Q_{HW}	Hot water energy	kW
Q_{CHW}	Chilled water energy	kW
Q_{CW}	Cooling water energy	kW
Rated	Adsorption chiller rated value	
DEI	Rated (design) chiller thermal energy input	
DC	Rated (design) chiller chilling capacity	
C_p	Specific heat capacity	kJ/kg.k
COP	Coefficient of performance	
CCHP	Combined cooling heating power	
Q_{Elec}	Total electrical power consumed	kW
Q	Thermal power	kW
$\dot{V}$	Volume flow rate	m^3/s
N	Number of data	
COPe	Total coefficient of performance	
u_y	Total uncertainty	%
TRN	TRNSYS simulation value	
Exp	Experimentally determined value	
Time	Time of day	Hour
ABS-PD	Absolute average percent	%

* Corresponding author e-mail: ahmad.sakhrieh@aurak.ac.ae

	deviation	
Mod	Model	
Act	Actual	
Pred	Predicted	
$\Delta\Delta t'$	Adapted characteristic equation method	
s', a, e and r	Parameters	
SS_r	Residual sum of squares	
SS_t	Total sum of squares	
R^2	Coefficient of determination	
RMSE	Root mean square error	
$\lvert\bar{\epsilon}\rvert$	Mean absolute difference	
CV	Coefficient of variation	%
y_i	Predicted value of the model	
$\hat{y}_i$	Associated measured value	
$\bar{y}_1$	Dependent variable mean	
Sec	Second	
Min	Minute	
Δ	Difference	
ρ	Density	kg/m^3
$\sum$	Summation	

1. Introduction

A high percentage of the electricity produced in Jordan is consumed in refrigeration and air-conditioning sector. The availability of solar radiation in phase with the seasonal and hourly cooling load profiles in most of the buildings in Jordan, in addition to the large share of primary energy consumed for air conditioning applications in buildings create a high motivation for the utilization of solar cooling technology for such type of buildings [1].Renewable energy can be considered an effective solution because it is a clean, environment friendly and inexpensive in the long term [2]. The present study focuses on one of the applications of solar energy, which is using solar energy as a heat source to power Solar Adsorption Refrigeration System (SARS).

A lot of interest has been revolving around the idea of using solar energy as an alternative source of energy at the present time. This is due to the environmental considerations currently arising all around the world [3-5]. Solar energy can be used as the main source to operate SARS, which can be driven by low-potential thermal power. This includes, but is not limited to solar energy, geothermal energy and wasted heat. Moreover, the working fluids of this system are environmentally friendly [6].

The use of the heat operated refrigeration system helps in reducing the environmental problems related to the use of HCFCs and CFCs as refrigerants, which are considered among the main causes for ozone layer depletion. Additionally, they directly contribute to the greenhouse effect [7]. Furthermore, the consumption of primary energy and the emission of greenhouse gases associated with electricity generation from fossil fuels lead to considerable environmental consequences and great economic costs.

Many research studies related to air conditioning by thermal driven solar cooling have been accomplished. Li and Wu [8] constructed a novel micro Combined Cooling, Heating and Power (CCHP) system, based on a two bed silica gel/water adsorption chiller. A comparison between simulation results and experimental data was conducted in order to propose a new model with an improved performance. Zhang *et al.* [9] presented a model of silica gel/water adsorption chiller powered by solar energy. Matlab-Simulink was used to simulate the operating conditions of the chiller. Rabhi *et al.* [10] carried out a simulation work on a solar adsorption chiller using silica gel as adsorbent and water as adsorbent. Also, the finite volume method was used to solve the system numerically. Effects of the average radius of the silica gel grain ranging from 0.6 mm to 0.9 mm and of the temperature regeneration ranging from 77°Cto 107°C were studied. Wang *et al.* [11] showed that a silica gel acts as a key role in adsorption refrigeration systems. It was found out that the silica gel/water adsorption refrigeration system is greatly influenced by the adsorption deterioration. Rezk *et al.* [12] used an empirical lumped analytical simulation model to study an adsorption cooling system with 450 kW two bed silica gel/water adsorption chillers. The results showed that the enhancement in the cooling capacity and System COP increased to reach maximum of 25% and 10%, respectively, upon increasing the fin spacing ratio of 2. Fasfous *et al.* [13] theoretically investigated the potential of utilizing a solar cooling system at The University of Jordan in Amman to improve the indoor air quality. They showed that proposed solar collectors of 40-m^2 areas could offer solar heat for an 8 kW solar air conditioning system. Solar heating (approx. 15–25% solar fraction) and domestic hot water (solar fraction up to 100%) could be also provided, with the solar air conditioning system. Lu *et al.* [14] used micro-porous silica gel–water and compound adsorbent of macro-porous silica gel/LiCl-methanol as working pairs in two adsorption cooling systems. The results indicated that the cooling capacity and COP are 1.0 kW and 0.13 respectively. Ali, et al. [15] developed a new adsorption air conditioning system driven by solar energy using silica gel/water adsorption chiller, heat exchanger, rotary desiccant and humidifier.

In Jordan, the application of the concept of solar cooling is not new. The review article of Ayadi *et al.* [16] mentioned three solar cooling systems utilizing concentrating collectors that were applied in Jordan; the first was by Hammad *et al.* who tested a prototype absorption chiller for air-conditioning by coupling the chiller to a prototype flat plate collector with a PTC collector in 1991 [17]; later, in 2000, a prototype PTC with an absorption chiller for refrigeration purpose in desert areas was tested [18]. In 2010, a 146 m^2 Parabolic trough collector was installed at the Dead sea hotel to supply the required heat for a 13 kW absorption chiller [16].

The first adsorption chiller installed in Jordan was a part of the Aqaba Residence Energy Efficiency (AREE) project funded by the EU-MED-ENEC program; it was installed and launched in June 2009 in a "green home". The solar cooling project is based on a thermally driven adsorption chiller, integrated in a cooling tower (water cooled system). Heat is supplied to the chiller by evacuated tube collectors. Based on above, and since the adsorption chillers require a lower supply temperature to the generator that can be easily produced by flat plate collector, flat plate solar collectors were used in this study to supply heat to the SARS which was installed at Hamdi Mango center for scientific research HMCSR–University of Jordan in Amman.

2. Theoretical Background

Solar cooling technology can be divided into three main categories: solar thermal cooling, solar electrical cooling and solar combined power and cooling. Thermal energy produced from the solar energy can be used in useful heating and cooling in the solar thermal cooling systems by thermo-physical or thermo-chemical processes. Solar thermal cooling is divided mainly into thermo-mechanical solar cooling and sorption technology [19].

Sorption refrigeration technology can be classified mainly into open sorption cycle and closed sorption cycle [20]. Open sorption cycle is classified into liquid or solid desiccant systems that are used for either humidification or dehumidification. Basically, there are two processes to transfer moisture from one air stream to another in the desiccant systems: desorption or regeneration process and sorption process. Liquid and solid desiccants behave under the same principle and hence their water vapor pressure is a function of moisture content and temperature.

Based on the sorption material, closed sorption cycles are divided mainly into liquid sorption and solid sorption. The liquid sorption refers to the absorption, while the solid sorption refers the adsorption. Absorption involves a liquid or solid sorbent that absorbs refrigerant molecules into its inside and changes either chemically and/or physically throughout the process. The most widely used working pairs in the absorption processes are lithium chloride-water, water-ammonia and lithium bromide-water. Adsorption, on the other hand, refers to a solid sorption process which a solid sorbent attracts refrigerant molecules onto its surface by chemical or physical force and without changing its form in the process [21]. Adsorption refrigeration process is achieved using a combination of adsorbent and adsorbate. Activated carbon-ammonia, activated carbon-methanol, activated carbon-ethanol, silica gel-water and zeolite-water are the most widely used working pairs in the adsorption processes.

The adsorption refrigeration cycle consists of two sorption chambers (Desorber and Adsorber), a condenser and an evaporator, as illustrated in Figure 1. The adsorption cycle achieves a COP ranging between0.3 to 0.7, depending upon the driving heat temperature, which in turn ranges between 55°Cand90°C. The adsorption chiller cycle consists of the following steps:

- In the desorber chamber, the refrigerant vapor is released by regenerating the solid sorbent which means desorb the refrigerant that cohesive on the surface by sorbent porous through applying the heat that is previously received from the heating source.
- The desorbed refrigerant is cooled and condensed to liquid in the condenser. Rejecting the heat through the cooling water supplied from a cooling tower does this.
- The cold refrigerant is vaporized under low partial pressure and low temperature in the evaporator while the useful cooling is produced.
- The refrigerant vapor then enters to the adsorber chamber from the evaporator and will be absorbed by the solid sorbent.
- The functions of two sorption chambers are reversed by alternating the opening of the butterfly valves and the direction of the heating and cooling refrigerants. In this way, the chilling refrigerant is obtained continuously. The cycle then repeats.

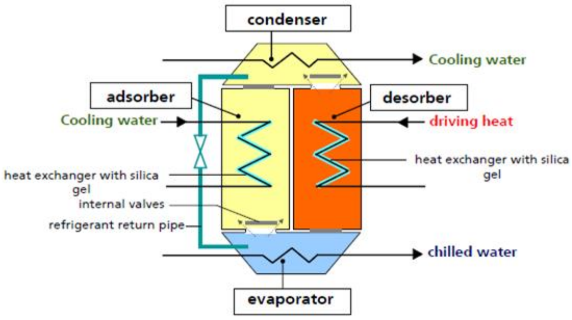

Figure 1. Schematic of adsorption cycle solar cooling system

The adsorption system operates under three temperature levels: high temperature used to supply the heat to the desorber, intermediate temperature used to reject heat in the condenser and adsorber, in addition to low temperature used in producing the coldness. Also there are two pressure levels in this system: high pressure at the condenser and low pressure at the evaporator.

There are many refrigerants that are used in adsorption refrigeration systems. Natural refrigerants include water (the most commonly used one) in addition to Ammonia. However, the most commonly applied refrigerants are methanol, ethanol, ammonia and water.

The thermal power of a chiller (Q) may be calculated from equation 1.

$$\dot{Q} = \dot{m}.\ Cp\ .\ \Delta T = \rho.\dot{V}.Cp\ .\ \Delta T \qquad (1)$$

where $\dot{m}$ (kg/s) is the mass flow rate of water, ρ(kg/m^3) is the density of water, $\dot{V}$(m^3/s) is the volume flow rate of water, Cp (kJ/kg.°C) is the specific heat capacity of water, and ΔT (°C) is the temperature difference of water stream.

The thermal instantaneous COP of the solar adsorption system of the solar adsorption system was calculated according to equation 2:

$$COP = Q_{CHW}/Q_{HW} \qquad (2)$$

where COP is the thermal coefficient of performance, Q_{CHW} (kW) is the chilling power, and Q_{HW} (kW) is the heating power.

The total COP (COP_e) of the solar adsorption system is the ratio of the chilling power of the system to the heating power and the total electrical power consumed, Q_{Elec}, of the system and was calculated according to equation 3:

$$COP_e = Q_{CHW}/(Q_{HW} + Q_{Elec}) \qquad (3)$$

The instantaneous Solar Fraction Cooling (SFC) of the solar adsorption is the ratio of the total chilling power of the system to the total cooling requirement and was calculated according to equation 4:

$$SFC = Q_{CHW,Total}/Q_{L,Total} \qquad (4)$$

where $Q_{CHW,Total}$ (kW) is the total chilling power of the system and $Q_{L,Total}$(kW) is the total cooling requirement.

The absolute average percent deviation (ABS-PD) was also calculated according to equation 4:

$$\text{ABS 4eal}\ \frac{1}{N_{data}}\sum_{0}^{N_{data}}\frac{|\text{Pred value lculated ac}|}{\text{Exp value}}.100\% \qquad (5)$$

where N is the number of data, predvalue is the predicted value, and expvalue is the experimental value.

The chilling capacity, Q_{CHW}, of the adsorption chiller at the prevailing conditions of inlet hot and cooling water temperatures, and the heat energy input, Q_{HW}, from hot water storage tank to the adsorption chiller were computed using equations 5 and 6.

$$Q_{CHW} = F_{DC} \, (Q_{CHWrated}) \tag{5}$$

$$Q_{HW} = F_{DEI} \, (Q_{HWrated}) \tag{6}$$

where F_{DC} is the design chilling capacity and F_{DEI} is the design energy input of the adsorption chiller model.

3. System Description

Silica gel/water SARS is installed to air condition in two connected laboratories in the ground floor of HMCSR building at The University of Jordan in Amman. HMCSR building consists of a ground floor and a basement with a total floor area of 2040 m^2.

The required cooling load of the two laboratories is 8 kW (2.27 ton refrigeration). The building envelope has no shading or double glassing [13]. Figure 2 shows the schematic diagram of the solar powered adsorption chiller.

Silica gel/water SARS basically consists of four subsystems, namely silica gel/water adsorption chiller, solar water heating unit, cooling tower and fan coil unit. There are some auxiliary components including; pipes, fittings, valves, pumps, expansion vessels and control unit(s).

An adsorption chiller with a nominal cooling capacity of 8 kW [22] was selected. The chiller has cold water storage tank with a capacity of 2000 L, cooling tower, fan coil unit, and some auxiliary components such as pipes, pumps and control unit(s) that were installed to supply the cold air to the two connected laboratories.

The solar adsorption system includes some components that contribute to the electricity consumption of the system, including; cooling tower, pumps and adsorption chiller. However, adsorption chiller as a thermally driven chiller consumes very low electrical power compared to a conventional vapor compression chiller. The total maximum electrical consumption of the whole system is 1616 W. The maximum electrical consumption of the six pumps, the cooling tower, and the adsorption chiller are 1069 W, 540 W, and 7.0 W, respectively. However, the electrical power consumption of the six pumps in the whole system (1069 W) is relatively high. This is attributed to the high pressure drop in circulation the thermal fluid inside the pipes of system, adsorption chiller, and collector absorber.

Flat plate solar collectors are the heat source of the system. Collectors are connected with a hot water storage tank through pipes and single speed pump within a closed circuit. The hot water storage tank was also connected with an adsorption chiller through pipes and single speed pump.

The cooling water unit consists of a flat plate heat exchanger and a cooling tower. Additionally, the flat plate heat exchanger was used to reduce the variation of the cooling water inlet temperature. In addition, the cooling tower was used to reduce the cooling water temperature by controlling the airflow rate. The flat plate heat exchanger, the cooling tower and the adsorption chiller were connected together using pipes and two single speed pumps within a closed circuit.

The Cold-water storage tank was connected to an adsorption chiller using pipes and single speed pump within a closed circuit in order to provide an infinitive cooling load to the adsorption chiller. The storage tank was also connected with a fan coil unit through pipes and single speed pump within a closed circuit in order to provide cold air to the two connected laboratories in HMCSR building. Some auxiliary components, including pipes, fittings, valves, expansion vessels and control unit(s) were installed to support the operation of the solar adsorption system.

The water inlet and outlet temperatures were measured by seven PT1000 platinum resistors. The temperatures of the working fluids were obtained under a steady state of operating conditions in which the solar adsorption system was operating under. The hot water, chilled water, and cooling water flow rate were measured using an ultrasonic flowmeter. Global solar radiation, ambient temperature, wet bulb temperature, relative humidity, and wind speed were measured using different sensors. Under these circumstances, data were recorded every two minutes. The technical specifications of sensors used for measuring of the performance of the solar adsorption system are displayed in table 1.

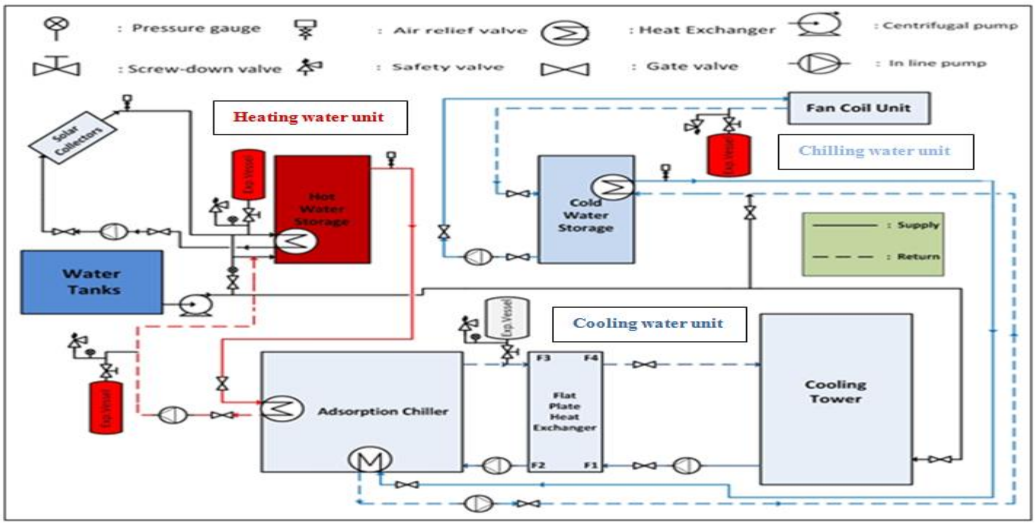

Figure 2. Schematic diagram of the solar powered adsorption chiller

Table 1. Technical specifications of sensors used for measuring of the performance of the solar adsorption system

Sensor type	Model	Specifications	
Flow rate	Ultrasonic flow meter	Flow range	Velocity: 0.1 – 9 m/s (0.3 – 30 ft/s)
		Accuracy	+ 2% full scale
		Temperature	Electronics: -28 to 140 °F (-20 to 60 °C) Transducer: -40 to 180 °F (-40 to 82 °C)
Temperature	PT-1000	Accuracy	At 0 °C, 0.3 °C and at 100 °C, 0.8 °C.
Global radiation	SOLRAD – Integrator (SOLRAD radiation indicator - Data logger)	Analogue inputs	1
		AD conversion resolution	1:10.000 bits
		Inaccuracy	< 0.1 %
		Operational temperature range	-10 to 40 °C
		Temperature accuracy, RMS	2 x 16 characters ºC
		Power supply	9 Volt battery
		Communication interface	RS-232
	Pyranometer**PMA 2144**	Response time	18 seconds (95%)
		Sensitivity change/year	< 1%
		Display resolution	1[W/m^2], 0.1[mW/cm^2]
		Operating environment	-40 to 175 °F (-40 to 80 °C), outdoor
		Angular response	2% for angels < 70°
Temperature **RH** **Wet Bulb** **Wind speed**	Datalogging / Printing Anemometer + Psychrometer Model: 451181	Accuracy	Temperature: ±1°F / °C RH: ±3% Wet Bulb: - Wind speed: ±3% rdg
		Range	Temperature: -4 to 144°F / -20 to 60 °C RH: 0 to 100%RH Wet Bulb: -7.6 to 158°F/-22 to 70°C Wind speed: 0.4 to 25 m/s
		Resolution	Temperature:0.1°F/°C RH:0.1% Wet Bulb: 0.1°C Wind speed: 0.1 m/s

4. Simulation

A TRNSYS simulation studio environment project was used to theoretically predict the performance of the whole solar adsorption system as shown in Figure 3. The black solid lines show the flow of system energy information. On the other hand, yellow solid lines show the flow of weather data information, while the green solid lines show the flow of the output information and the brown dotted lines show the flow of control strategy information.

The main components in the TRNSYS simulation project are: Type 4a – Hot water storage tank, Type 3b – Pump, Type 73 – Theoretical flat plat solar, Type 51b – Wet cooling tower and Type 107 – Absorption chiller that were used to predict the thermal performance of the whole solar adsorption system for different periods of the year. However, an inbuilt Type 107 was used as an adsorption chiller component. A more detailed control strategy was used in this case to replicate the real operation of the solar adsorption system.

A summary of the characteristics and key inputs for the different TRNSYS components used in the simulation of solar adsorption system are listed in table 2.

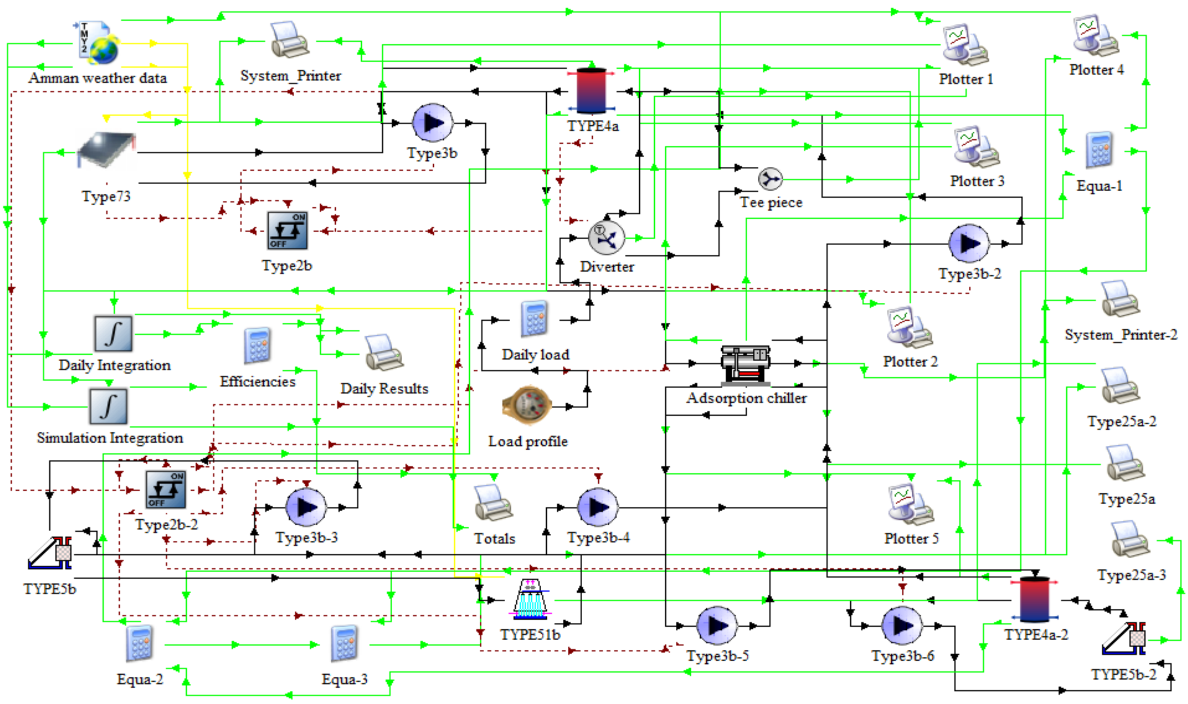

Figure 3. TRNSYS project for simulation of the solar adsorption system

Table 2. Parameters and key inputs of TRNSYS model

TRNSYS type	Key input	Value	Unit
Type 4a – Hot water storage tank	Fluid specific heat	4.19	kJ/kg.k
	Fluid density	1000	kg/m^3
	Loss coefficient	1.0	$kJ/hr.m^2.k$
	Tank volume	2000	Liters
	Number of temperature levels (Nodes)	8	-
Type 3b – pump:(1,2), (3) and (4)	Maximum flow	(1600), (3700) and (2000)	kg/hr
	Maximum power	882	kJ/hr
	Conversion coefficient	0.0	-
	Fluid specific heat	4.19	kJ/kg.k
	Power coefficient	0.5	-
Type 73 – Theoretical flat plat solar collector	Number in series	8	-
	Fluid specific heat	4.19	kJ/kg.k
	Incidence angle	45	degrees
	Collector area	59.064	m^2
Type 107 – Modified Adsorption chiller	Rated COP	0.60	-
	Rated chilling capacity	28800	kJ/hr
	Fluid specific heat capacity	4.19	kJ/kg.k
	Chiller on and off signal	1 or 0	-
	Auxiliary electrical power	25.2	kJ/hr
Type 4a – Cold water storage tank	Fluid specific heat	4.19	kJ/kg.k
	Fluid density	1000	kg/m^3
	Loss coefficient	1	$kJ/hr.m^2.k$
	Tank volume	2000	Liters
	Number of temperature levels (Nodes)	1	-
Type 51b – Wet cooling tower	Fan maximum power	1836	kJ/hr
	Maximum air flow rate	81.60	m^3/hr
	Number of tower cells	1	-
	Mass transfer coefficient	2.3	-
	Mass transfer exponent	-0.72	-
Type 5b – Heat exchanger	Specific heat of hot side fluid	4.19	kJ/kg.k
	Specific heat of cod side fluid	4.19	kJ/kg.k

5. Experimental Setup

Experimental results and measurements of system performance were carried out during the months of May and June at the University of Jordan. Eight different days were selected to study the performance of the solar adsorption system. Clear sky and partly cloudy are the prevalent weather conditions at the location of the experimental setup. Figure 4 shows the solar adsorption system that was installed at HMCSR. The hot water, the chilled water and the cooling water systems were adopted as three water supply systems of solar adsorption system. Different sensors were installed in each water supply system. The baseline parameters of the solar adsorption system in -different locations of experimental setup are given in Table 3. It can be seen that the functions of two sorption chambers are reversed by alternating the opening of the butterfly valves and the direction of the heating and cooling refrigerants through increasing temperature in one sorption chamber and decreasing temperature in the other sorption chamber at the same time.

Figure 4. Solar adsorption system

Table 3. Measured data of the solar adsorption system

Time [min]	G.S.R [W/m^2]	R.H [%]	Wind [m/s]	T amb [°C]	T A OUT [°C]	T D OUT [°C]	T LT IN [°C]	T LT OUT [°C]	T MT OUT [°C]	T LT Ext [°C]	T HT Ext [°C]	T1 OUT [°C]	dQ LT [kW]
00:00	1051	19.0	0.6	31.7	37.3	80.2	23.7	20.8	36.9	23.5	80.0	96	4.3
02:00	1046	19.3	0.9	31.1	33.2	80.9	23.6	20.7	32.8	23.4	80.1	96	4.3
04:00	1049	19.2	0.5	31.5	29.6	82.1	23.6	21.5	30.1	23.3	80.1	96	4.3
06:00	1053	19.8	0.6	31.4	61.7	58.3	23.6	20.8	38.1	23.3	80.0	96	4.2
08:00	1048	19.9	0.4	31.2	80.9	36.3	23.4	21.2	36.2	23.3	79.7	96	4.2
10:00	1060	20.7	0.6	30.9	83.3	31.5	23.4	20.0	31.1	23.1	79.5	96	4.2
12:00	1041	21.1	0.5	30.8	84.1	28.7	23.3	20.1	29.1	23.1	79.5	96	4.1
14:00	1067	19.9	0.5	31.5	36.6	82.3	23.3	20.1	36.1	23.0	79.5	96	4.1
16:00	1046	20.2	0.6	30.8	33.8	84.6	23.3	20.5	32.9	23.0	79.2	97	4.1
18:00	1051	20.5	0.4	30.6	30.9	87.7	23.2	21.6	30.5	23.0	79.5	97	4.1
20:00	1062	21.4	0.5	30.7	61.5	51.3	23.2	21.2	33.0	22.9	79.9	97	4.5
22:00	1090	20.6	1.1	30.3	85.8	37.0	23.1	20.7	36.6	22.7	80.2	98	4.5
24:00	1039	19.5	0.8	30.6	88.3	32.4	23.0	21.6	31.2	22.7	80.4	98	4.5
26:00	1061	20.3	0.8	31.2	51.3	62.1	23.0	21.7	38.0	22.6	80.6	98	4.1
28:00	1047	19.3	0.5	31.3	35.1	83.0	22.8	20.6	34.9	22.5	80.8	98	4.1
30:00	1087	18.8	2.1	31.0	32.3	83.9	22.7	20.9	31.9	22.5	81.0	98	4.1

G.S.R: Global solar radiation [W/m2]
R.H: Relative humidity [%]
T amb: Ambient temperature [°C]
T A OUT: Temperature of the adsorber chamber at the adsorption chiller [°C]

T D OUT: Temperature of the desorber chamber at the adsorption chiller [°C]
T LT IN: Temperature of the chilled water at the chiller inlet [°C]
T LT OUT: Temperature of the chilled water at the chiller outlet [°C]
T MT OUT: Temperature of the cooling water at the chiller outlet [°C]

T LT Ext: Water temperature of the cold water storage tank [°C]
THT Ext: Water temperature of the hot water storage tank [°C]
T1: Collectors outlet temperature [°C]
dQ LT: Chilling capacity [kW]

5.1. Uncertainties Measurement

The variable y is measured indirectly by measuring the independent variables, x_1, x_2, x_3,……..x_m, where y is a function of independent variables as y = f (x_1, x_2, x_3,……..x_m). The uncertainties u_1, u_2, u_3,……..u_m in x_1, x_2, x_3,……..x_m, respectively, are used to give the total uncertainty in y, u_y according to equation 7.

$$u_y = \sqrt{\sum_{j=1}^{m} \left(\frac{\partial y}{\partial x_j}\right)^2 \quad u_j} \tag{7}$$

Equation 1 and equation 7 are used to give the relative uncertainty in the instantaneous thermal power, Q, measured according to equation 8. The sum of the uncertainties in the instantaneous powers was calculated to give the total uncertainty [23]:

$$\frac{u_Q}{Q} = \sqrt{\left(\frac{u_\rho}{\rho}\right)^2 + \left(\frac{u_{\dot{V}}}{\dot{V}}\right)^2 + \left(\frac{u_{C_p}}{C_p}\right)^2 + \frac{{u_{T_1}}^2 + {u_{T_2}}^2}{(T_2 - T_1)^2}} \tag{8}$$

where $u_Q, u_\rho, u_{\dot{V}}, u_{C_p}, u_{T_1}$ and u_{T_2} are the uncertainties inthe thermal power measured, water density, volume flow rate, water specific heat, lower and upper temperatures of the water, respectively.

Figure 5 shows the results of measurements of the thermal power measured. The figure contains error bars indicating the extents of uncertainties. It is observed that the measurements of chilling power, heating power and cooling power have high values of uncertainty at an average between 5.3% and 9.1%.

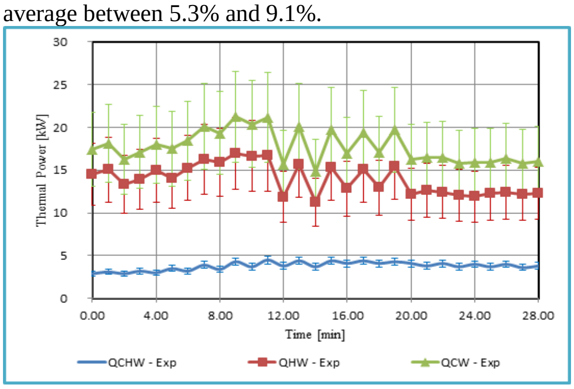

Figure 5. Chiller thermal powers and measurement uncertainties

6. Results and Analysis

Theoretical simulation was basically carried out using TRNSYS simulation software. Figure 6 shows the predicted thermal power of the flat plate solar collectors with respect to the collector slopes on May20th.

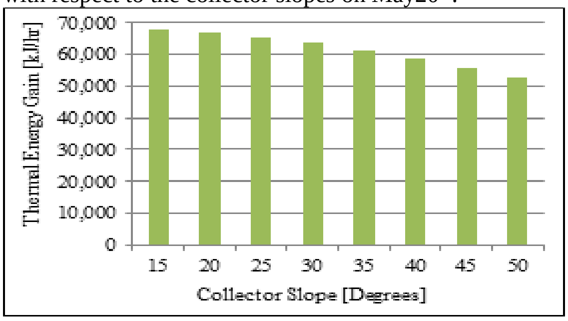

Figure 6. Collector thermal gain for different collector tilts (Simulations on May20th)

Figure 7 displays the different values of the total thermal power collected at different collector tilts during the months of May and June. From Figure 5, it is evident that the 15° collector slope performs better than all the other collector tilts on 20th, May. Precisely, the optimum tilt angle during this period is observed from Figure 7 to be 15°. However, it is also clear that the difference in the total thermal power collected between the tilts of 0.0° to 35° is very minute, and therefore, any convenient tilt with in this range gives an adequate performance during this period.

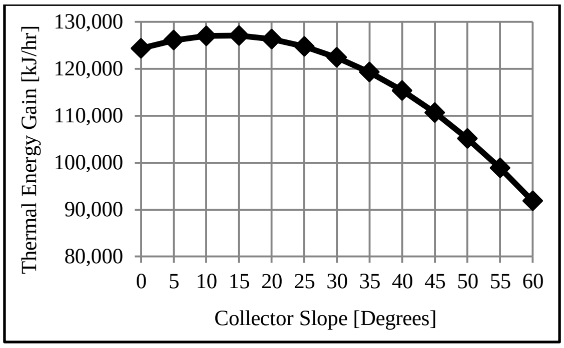

Figure 7. Thermal power gain for more different collector tilts

The simulation model was validated for further simulation campaigns aiming at defining the best operating points of the solar adsorption system and tracing a path towards the plant performance improvement.

Operating temperatures of heating, cooling and chilled water influence the chiller performance. The flow rate of heated, cooled and chilled water is also one of the operating parameters that influence the chiller performance. Therefore the effect of operating conditions on the performance of simulated chiller is important to determine the conditions that can increase the output of the chiller. The chiller performance at the design operating conditions will be used as the baseline for comparison and these listed in Table 4.

Table 4. Adsorption chiller reference operating conditions at design operation

Operating Condition	Value	Unit
Heating water inlet temperature	80	°C
Cooling water inlet temperature	27	°C
Chilled water inlet temperature	18	°C
Heating water flow rate	1531.5	l/h
Cooling water flow rate	3475.5	l/h
Chilled water flow rate	1896.1	l/h

Figure 8 compares the predicted heated, cooled and chilled water outlet temperatures and their actual analogous values, which were supplied by the manufacturer based on the same average inlet conditions. Table 5 presents the absolute average percent deviation (ABS-PD) for heated, cooled and chilled water outlet temperatures for the test results shown in Figure 8. The deviation between the predicted COP, heating power and chilling capacity are also presented. It is known that the predicted values of thermal simulation models can be accepted if the ABS-PD is below 30% [21].Table 5 and Figure 8 indicate clearly the good agreement between the model and experimental results.

Table 5. Simulation model deviation analysis ($\dot{m}_{HW}$ = 1600 l/h, $\dot{m}_{CW}$ = 3700 l/h, $\dot{m}_{CHW}$ = 2000 l/h)

Term	ABS-PD [%]	Term	ABS-PD [%]
T_{HWout}	2.8	Q_{HW}	11.5
T_{CWout}	3.9	Q_{CHW}	14.8
T_{CHWout}	17.4	COP	3.7

Table 6 presents the ABS-PD for average heating, cooling and chilled water outlet temperature in addition to heating power, chilling capacity and COP for different experimental runs. It can be seen that the maximum absolute percent deviation calculated based on steady state cycle is 19.3%.

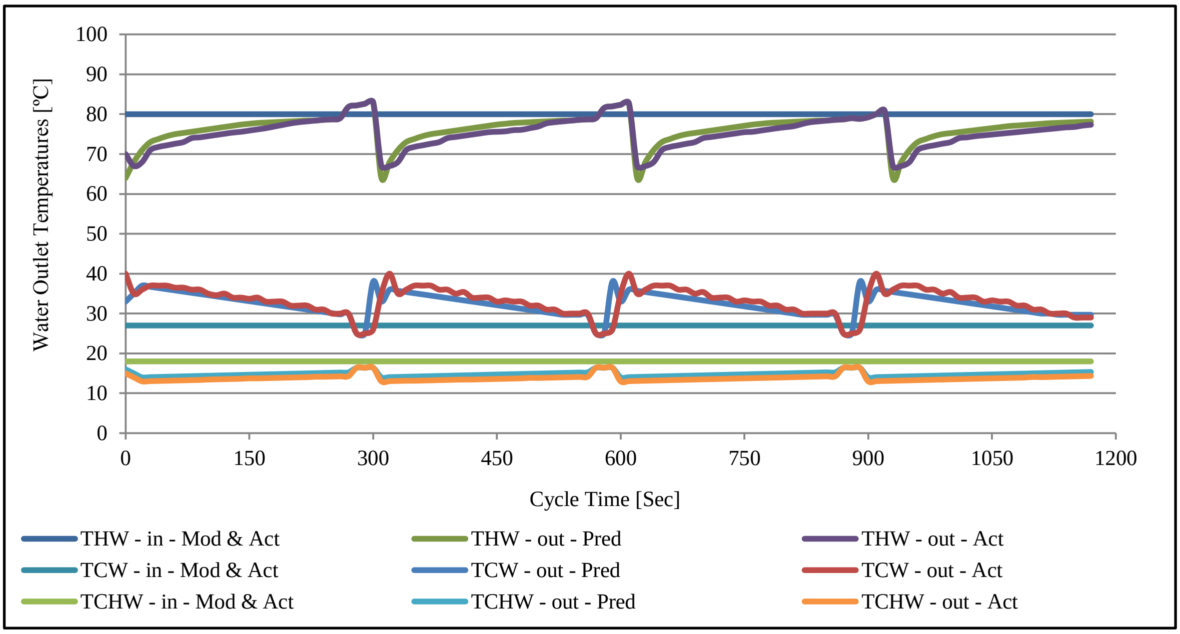

Figure 8. Comparison between predicted data and actual data

Table 6. Simulation model deviation analysis at one steady state cycle

Term	RUN-1		RUN-2		RUN-3		RUN-4		Unit
$\dot{m}_{HW}$	1531.5		1531.5		1531.5		1531.5		l/h
$\dot{m}_{CW}$	3475.5		3475.5		3475.5		3475.5		l/h
$\dot{m}_{CHW}$	1896.1		1896.1		1896.1		1896.1		l/h
$T_{HWin,avg}$	80.5		79.8		80.2		80.3		°C
$T_{CWin,avg}$	27.5		27.4		27.2		27.6		°C
$T_{CHWin,avg}$	18.1		18.1		18.1		18.2		°C
Deviation analysis (actual temperature & ABS-PD)									
T_{HWout}	74	1.1	73	1.9	73.2	1.4	73.8	1.7	°C & %
T_{CWout}	32.3	0.8	32.1	1.2	31.9	1.1	32.4	0.5	°C & %
T_{CHWout}	16.4	13.7	16.3	13.4	16.2	12.7	16.5	14.1	°C & %
Q_{HW}	12	11.1	12.7	11.4	13.1	11.5	12	10.9	°C & %
Q_{CHW}	4	15.1	4.2	15.8	4.5	19.3	4	15.3	°C & %
COP	0.33	4.1	0.33	4.3	0.34	8.1	0.33	4.2	°C & %

Cooling and heating water inlet temperature influences adsorption chiller performance. Decreasing cooling water inlet temperature not only increases chilling capacity, but also enhances the COP adsorption chiller, due to the significant increase in adsorption rate. Increasing heating water temperature also enhances chiller chilling capacity due to enhance desorption rate. However, it negatively influences the chiller COP depending on the cooling water inlet temperature. As a result, the generation temperature lift, defined as the difference between heating and cooling water inlet temperatures, was calculated and used in the investigation. It is noteworthy to mention that the chilled water inlet temperature depends mainly on the application and hence it was kept constant at its design value.

Figure 9 shows the change in chiller chilling capacity versus generation temperature lift at various cooling water inlet temperatures. Other operating conditions, such as cycle time and secondary fluid flow rate, remained constant at their design values. As the generation temperature lift increases the chiller chilling capacity increases for all cooling water inlet temperatures. In Figure 8, the experimental results at the operating conditions as shown in Table 6 are presented with good agreement with the model.

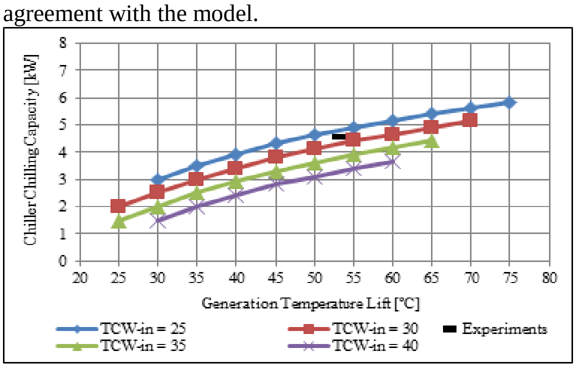

Figure 9. Generation temperature lift influence on chiller performance

Figure 10 depicts the variation in the chiller COP with generation temperature lift. It is observed that at low cooling water temperature, the chiller COP decreased with increasing the generation temperature lift within the tested range. However, at a higher temperature for cooling water (TCW>30°C), the chiller' COP initially increased to a certain point and then remained relatively constant with the increase in the generation temperature lift. The decrease in chiller COP at low generation temperature lift and high cooling water temperature is due to the insufficient refrigerant circulation required to generate the cooling power. On the other hand, the decrease in chiller COP at high temperature lift is due to the increase in heat losses.

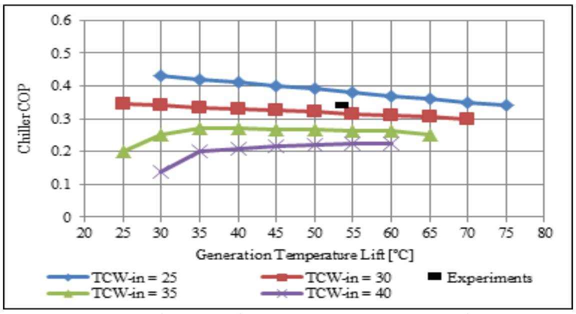

Figure 10. The influence of generation temperature lift on chiller COP

The variation of chiller COP with the generation temperature lift can be used as a load control tool. For example, at cooling water temperature of 35°C, the chiller chilling capacity increased almost linearly (from 2.9 to 4.4kW) with increasing the generation temperature lift (from 40°C to 65°C). The reduction in chiller COP (from 0.27 to 0.25) is relatively small.

7. Conclusions

In the present work, the performance of solar adsorption system under Jordanian climate conditions was simulated using TRNSYS and simulation results were validated against experimental results. The experimental investigation for an 8.0 kW solar adsorption refrigeration system installed at the roof of Hamdi Mango center at the University of Jordan in Amman shows that the Coefficient of Performance (COP) was in the range from 0.14 to 0.34 which is less than the designed theoretical value of 0.55. The measured parameters include the ambient temperature, global solar radiation, relative humidity, wind speed and the temperatures of the solar adsorption system at different locations. The collected data were carried out during two months, which are May and June, and further measurements were needed to measure the system performance during summer time in July and August in addition to the system performance during the whole year. Also, further investigations for system performance will be carried out for different values of the average chilled water outlet temperature, cooling water inlet temperature, and hot water inlet temperature.

Also, simulation of the solar adsorption system has been carried out using the TRaNsientSYstem Simulation software (TRNSYS). All in all, it was found that the actual measurements indicate that a chilling power of solar adsorption system is on the average of 65% lower than the theoretical simulation predictions. This is attributed to a number of key reasons such as; high level of uncertainty in the hot water energy and cooling water energy measurements due to the temperature measuring sensors having a low accuracy, and the difference between theoretical and actual tank loss coefficient.. The simulation model was validated for further simulation campaigns aiming at defining the best operating conditions of the solar adsorption system and tracing a path towards the plant performance improvement. The chilling capacity has a maximum absolute percent deviation calculated based on steady state cycle of 19.3%.

In general, it was found that the simulation results under predicts the actual ones. This is attributed to a number of key errors faced throughout the research, such as heat losses in the whole system, water leakage in the cooling tower and solar collectors, and high pressure drop in circulation the thermal fluid inside the pipes of system, adsorption chiller, and collector absorber. Therefore, the measured data for solar cooling system needs to be collected continuously for longer periods and for different hot and cold water temperatures in addition to the reduction of the key errors mentioned above and then the measured data can be compared again with the simulated results to get more agreement results.

Acknowledgements

The authors of this paper would like to thank the deanship of scientific research in The University of Jordan for their support in conducting this research work.

References

[1] Ayadi. O, Mauro. A, Aprile. M, Motta. M, 2012, Performance assessment for solar heating and cooling system for office building in Italy. Energy Procedia Volume30, 2012, Pages 490–494.

[2] Sembatya M. Performance evaluation of a solar cooling system in UAE - Ras Al Khaimah by both experiment and simulation, M.S. thesis, University of Gävle, Sweden, 2013.

[3] ChenC. J., WangR. Z. , XiaZ. Z. , KiplagatJ. K. , LuZ. S. Study on a compact silica gel-water adsorption chiller without vacuum valves: Design and experimental study.App. Energy 2010; 87 (1): 2673-81.

[4] Ahmad Sakhrieh, Waleed Shreim, Hatem Fakhruldeen, Hasan Hasan, Ahmed Al-Salaymeh, Combined Solar-Geothermal Power Generation using Organic Rankine Cycle, Jordan Journal of Mechanical and Industrial Engineering, Volume 10 (1), pp. 1-9, 2016.

[5] Bashar K. Hammad, Shaher M. Rababeh, Mohammad A. Al-Abed and Ahmed M. Al-Ghandoor, Performance Study of On-Grid Thin-Film Photovoltaic Solar Station as a Pilot Project for Architectural Use, Jordan Journal of Mechanical and Industrial Engineering, Volume 7 (1), pp 1-9, 2013.

[6] Al-GhoutiA., Yousef I., Ahmad R., GhrairA. M., Al-MaaitahA. Characterization of diethyl ether adsorption on activated carbon using a novel adsorption refrigerator. Chem. Eng. Journal 2010; 162 (1): 234-41.

[7] BaijuV., MuraleedharanC. Performance study of a two stage solar adsorption refrigeration system. Inter. Journal of Eng. Science and Tech. 2011; 3 (7): 5754-64.

[8] LiS., Wu J. Y. Theoretical research of a silica gel-water adsorption chiller in a micro combined cooling, heating and power (CCHP) system.App. Energy 2009; 86 (6): 958-67.

[9] ZhangG., WangD. C., Zhang J. P., Han Y. P., Sun W. Simulation of operating characteristics of the silica gel-water adsorption chiller powered by solar energy.Sol. Energy2011; 85 (7):1469-78.

[10] Rabhi K., Ali C., Ben BachaH. Numerical study of combined heat and mass transfer in the silica gel-water adsorption chiller. Inter. Review of Mech. Eng. 2012; 6 (6).

[11] Wang D., Zhang J., Xia Y., Han Y., Wang S. Investigation of adsorption performance deterioration in silica gel-water adsorption refrigeration.Energy Conv. and Manag.2012; 58: 157-62.

[12] Rezk A., Al-Dadah R. K., Mahmoud S., Elsayed A. Effects of contact resistance and metal additives in finned-tube adsorbent beds on the performance of silica gel/water adsorption chiller.App. Thermal Eng.2013; 53 (2): 278-84.

[13] Fasfous A., Asfar J. , Al-Salaymeh A., Sakhrieh A., Al_hamamre Z., Al-bawwab A., HamdanM. Potential of utilizing solar cooling in The University of Jordan.Energy Conv. and Manag. 2013; 65: 729-35.

[14] Lu Z., Wang R., Xia Z., Gong L. Experimental investigation adsorption chillers using micro-porous silica gel-water and compound adsorbent-methanol.Energy Conv. and Manag. 2013; 65: 430-7.

[15] Ali C., Rabhi K., Nciri R., Nasri F., Ben Bacha H. New adsorption air conditioning system powered by solar energy; operation principals and winter mode modelling and simulation.Inter. Review of Mech. Eng. 2013;7 (1).

[16] Ayadi O., Aprile, M. Motta, M. Solar cooling systems utilizing concentrating solar collectors -An overview. Energy Procedia 2012; 64(3).

[17] Hammad M., Audi M. Performance of a solar LiBr-water absorption refrigeration system. Renewable Energy 1992; 2(3).

[18] Hammad M and Habali S. Design and performance study of a solar energy powered vaccine cabinet. Applied Thermal Engineering 2000; 20(18).

[19] Hwang Y., Radermacher R., Al Alili A., Kubo I. Review of solar cooling technologies.HVAC&R Research2008; 14 (3): 507-28.

[20] Saudagar R. T., Ingole P. R., Mohod T. R., Choube A. M. A review of emerging technologies for solar air conditioner, International Journal of Innovative Research in Science, Eng. and Tech. 2013; 2 (6).

[21] Al-Fasfous A. Investigation of the performance of the adsorption solar air conditioning systems under Jordanian climate conditions. M.S. thesis, Department of mechanical Engineering, The University of Jordan, Jordan, 2012.

[22] Daßler I., Mittelbach W. Solar cooling with adsorption chillers. Energy Procedia 2012; 30: 921-9.

[23] Semyon G. Rabinovich. Evaluating measurement accuracy, a practical approach. 4th ed. Springer, USA; 2010.